Journal of
Synchrotron
Radiation

ISSN 0909-0495

Received 14 February 2011
Accepted 24 June 2011

In situ multi-axial loading frame to probe elastomers using X-ray scattering

Yannick Pannier,[a] Henry Proudhon,[a] Cristian Mocuta,[b] Dominique Thiaudière[b] and Sabine Cantournet[a]*

[a]Centre des Matériaux, Mines Paritech, UMR CNRS 7633, 91003 Evry, France, and [b]Synchrotron Soleil, L'Orme des Merisiers, BP 48, 91192 Gif sur Yvette, France.
E-mail: sabine.cantournet@mines-paristech.fr

An *in situ* tensile–shear loading device has been designed to study elastomer crystallization using synchrotron X-ray scattering at the Synchrotron Soleil on the DiffAbs beamline. Elastomer tape specimens of thickness 2 mm can be elongated by up to 500% in the longitudinal direction and sheared by up to 200% in the transverse direction. The device is fully automated and plugged into the *TANGO* control system of the beamline allowing synchronization between acquisition and loading sequences. Experimental results revealing the evolution of crystallization peaks under load are presented for several tension/shear loading sequences.

Keywords: natural rubber; X-ray diffraction; multi-axial loading; crystallization.

1. Introduction

Elastomer materials possess an interesting self-reinforcement character owing to their ability to crystallize under loading. This property, called strain-induced crystallization, is of particular importance for the final mechanical properties of these materials. X-ray diffraction is therefore a natural tool for studying the evolution of the crystalline phase under load.

Several *in situ* deformation studies of natural rubber have been carried out in the past. Since the pioneering work of Treloar (1947), various authors have studied the stress-induced crystallization of pure vulcanized rubbers. As reported by Gent (1954) and by Thomas (1955), the strain-induced crystallization effect in natural rubber (NR) based materials would explain its excellent mechanical properties, in particular its resistance to crack propagation. Polymer chain crystallization in NR-based materials slows down the crack propagation, giving the material its high tensile strength. Flory (1953) noted that the hardening observed in pure NR could be due to the formation of crystallites, these particles playing the key role of reinforcement particles.

Recently, Albouy *et al.* (2005) and Toki *et al.* (2006) investigated the effective local deformation in stretched carbon black (CB) filled NR by *in situ* X-ray measurements during uni-axial deformation. Another aspect investigated by Toki *et al.* (2006) and Trabelsi *et al.* (2004) using wide-angle X-ray scattering (WAXS) was the evolution of the crystallite sizes *versus* strain in the case of CB-filled NR.

Despite its importance for industrial applications, the study of multi-axial strain induced crystallization by *in situ* synchrotron X-rays has never been reported. Several bi-axial testing devices have already been produced as reported by Brieu & Diani (2007), Marco & Chevalier (2008) and Geandier *et al.* (2010), but none of these allow samples to be deformed by more than the 250% needed to observe crystallization in NR-based materials. Bi-axial testing is also not very well suited for very large strains owing to the heterogeneous stress field usually obtained in cross-shaped specimens. In addition, it is worth noting that bi-axial testing does not involve any rotation of the principal stress axes. It would then be difficult to generalize the observed material behaviour to multi-axial loading.

The objective of the present work is to analyze mixed tensile–shear tests and track the evolution rate and the orientation of the crystallite induced by the multi-axial loading. Because crystallization and melting of crystallites are strongly time dependent, real-time analysis is critical to limit relaxation processes. The evolution of the crystallites' orientation distribution during *in situ* loading will be derived from the analysis of two-dimensional WAXS patterns. These measurements are key to understanding the underlying coupling between crystallization and deformation mechanisms.

2. Specific requirements for testing elastomers under WAXS

The objective of our experiment is to link elastomer multi-axial mechanical behaviour with stress-induced crystallization. This requires imposing and measuring precisely a multi-axial stress state in the specimen and following the crystalline microstructure evolution in real time using WAXS. Multi-axial mechanical tests on elastomers under WAXS combine several difficulties owing to elastomer viscosity and high strain

capability. Thus, *in situ* synchrotron X-ray diffraction measurements can be used favourably to study strain-induced crystallization under multi-axial loading owing to a very small spot size and a high flux of photons. In addition, to characterize both crystallization kinetics and morphology (crystallites sizes and orientation), a way of recording two-dimensional WAXS patterns rapidly is necessary.

The spot size must be small enough to avoid any stress gradient averaging in the analysis area (*i.e.* in the whole region interacting with X-rays). In the case of uni-axial tests the stress is homogeneous over a large area, but this is more intricate in the case of a multi-axial loading. Most multi-axial tests with elastomers are conducted on dog-bone-shaped axisymmetric specimens strained in mixed tension/torsion mode. In this case the stress varies with the distance from the surface of the specimen and it would be difficult to operate X-ray scattering with a unique and homogeneous area of matter. Therefore, a symmetric flat specimen loaded mechanically in its plane is a good way to obtain a homogeneous stress state in the thickness probed by X-rays in transmission mode.

Elastomers exhibit high relaxation sensibility, so interrupted tests lead to an underestimated stress state. Owing to high flux and motorized mechanical testing devices, it is possible to load the specimen continuously by imposing a constant displacement speed. The imposed velocity should be small enough to guarantee weak strain evolution during the exposure time of the area detector (typically 1 s) with a reasonable total test duration. With a low enough exposure time (about 1 s with a MAR345 image plate and 2 mm-thick NR specimens) it is also possible to study the relaxation process.

Elastomers also exhibit large deformation capabilities: natural rubber crystallizes near 250% and can be typically elongated until 600% before failure, making it difficult to analyze the same area during the test. One solution is to apply symmetric displacements of the grips, keeping the central zone of the specimen in a fixed position. The design of the specimens suffers some additional constraints. One of them is the minimum thickness of the specimen, which should be sufficient to obtain a uni-axial stress state. To respect dimension ratios leading to a homogeneous tensile–shear stress state in the central zone, the elastomer sample should be at least 100 mm long by 20 mm wide and 2 mm thick. Combining these dimensions with several hundreds of percent elongation can seem difficult to achieve using a compact testing device. The following section presents a testing machine, that we named TRACY, which meets all of those requirements.

3. Technical characteristics of the mixed tensile–shear loading device

The in-house-developed *in situ* device should be small and light enough to be integrated into a WAXS set-up of a synchrotron beamline like DiffAbs at Synchrotron Soleil. Motorization and automation of the system is required to ensure a continuous multi-axial loading synchronized with regular acquisition of diffraction patterns during the loading path. The proposed system will impose mixed tensile–shear loads independently to study non-proportional multi-axial load paths.

The mechanical testing device (see Fig. 1) is a tensile–shear device on elastomer tape specimens 100 mm long and about 2 mm thick. The tensile motion is ensured by two symmetrical rolling grips with rectangular holes to hold the specimen. These rollers are driven by a stepper motor, worm gears and a synchronous belt. To block the elastomer tape in the roller holes, 1 mm-thick plates clamp the ends with set screws. The 20 mm-diameter rollers are driven in opposite directions. In this way the first turn leads to about 200% elongation of the specimen. Calibration curves, depending on the material and on the width of the specimen, were produced to relate elongation (measured with a laser extensometer) as a function of the roller rotation angle (see Fig. 3*e*).

Shear load is applied owing to lateral symmetric clamps featuring a vertical gap of 4 mm (this distance can be reduced but edge effects may appear). When the specimen is elongated in tension, symmetric holders clamp the specimen owing to two steel plates screwed onto the carriages (Fig. 1, label 2). The carriages move in opposite directions owing to lead screws driven symmetrically by a second stepper motor and worm gears. With this set-up it is only possible to shear the specimen perpendicularly to the elongation direction. Nonetheless, these paths are non-proportional, and multi-axial-induced crystallization can be studied.

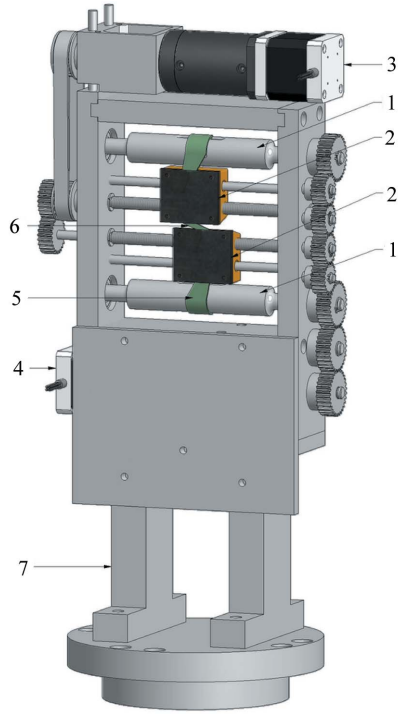

Figure 1
Description of the tensile–shear loading device TRACY. 1, roller-shape tension grips with rectangular drilled hole; 2, shear grips driven in opposite directions by two lead screws; 3, stepper motor powering lead screws of shear grips; 4, stepper motor driving roller-shape tension grips; 5, elastomer specimen strained in mixed tension–shear mode; 6, analysis area in the middle part of the illuminated specimen; 7, fixture to adapt the machine onto the diffractometer.

A fixture was designed to adapt the machine to the DiffAbs beamline diffractometer (the diffractometer is used here only to automatically rotate the stage for multi-modal imaging) and pre-position the centre of the specimen in the X-ray beam (Fig. 1, label 7). A fine-tuning of the specimen position in the X-ray beam is then achieved using a motorized translation of the diffractometer, carrying the tensile–shear loading device. The whole set-up is designed such that the probed area of the sample does not shift (laterally or vertically) in the X-ray beam.

The stress state in the specimen during shear load is not homogeneous, mainly owing to the boundary conditions. Optical strain field measurement in the centre of the specimen is then necessary to assess the shear magnitude in the X-ray illuminated zone. The technique is based on the acquisition of surface images of the specimen using a CCD camera which are then processed using a digital image correlation (DIC) algorithm. To ensure contrasted and convected patterns onto the surface, a specific marking technique is used. Because of a limited optical depth of field, it is necessary to ensure perpendicularity of the specimen with optical axes of the camera.

To place the specimen perpendicularly to the X-rays during the 1 s acquisition, an automatic sequence was implemented in data acquisition routines to synchronize rotation of the machine, DIC image acquisition, beam illumination, diffraction pattern acquisition and multi-axial loading of the specimen (*cf.* Fig. 2).

The procedure to load a specimen in mixed tensile–shear mode is illustrated in Fig. 3 and is as follows.

(i) The elastomer tape specimen extremities are introduced and fixed in roller holes. Rollers are adjusted to apply zero strain and a reference WAXS image is taken; note the reflective markers stuck onto the specimen.

(ii) The specimen is then elongated continuously until several hundreds of percent longitudinal strain is reached. Strain is measured with a laser extensometer using the reflective markers. WAXS images are taken sequentially and synchronized with the elongation measurements (see Fig. 2).

(iii) When the desired elongation is achieved, steel plate clamps, bonded with elastomer sheets for maximum adherence, are used to pin the specimen elongated and are screwed onto shear carriages.

(iv) Motor-driven carriages move in opposite directions and the specimen can be sheared up to 200% depending on previous tensile loading. The strain field is measured simultaneously by DIC.

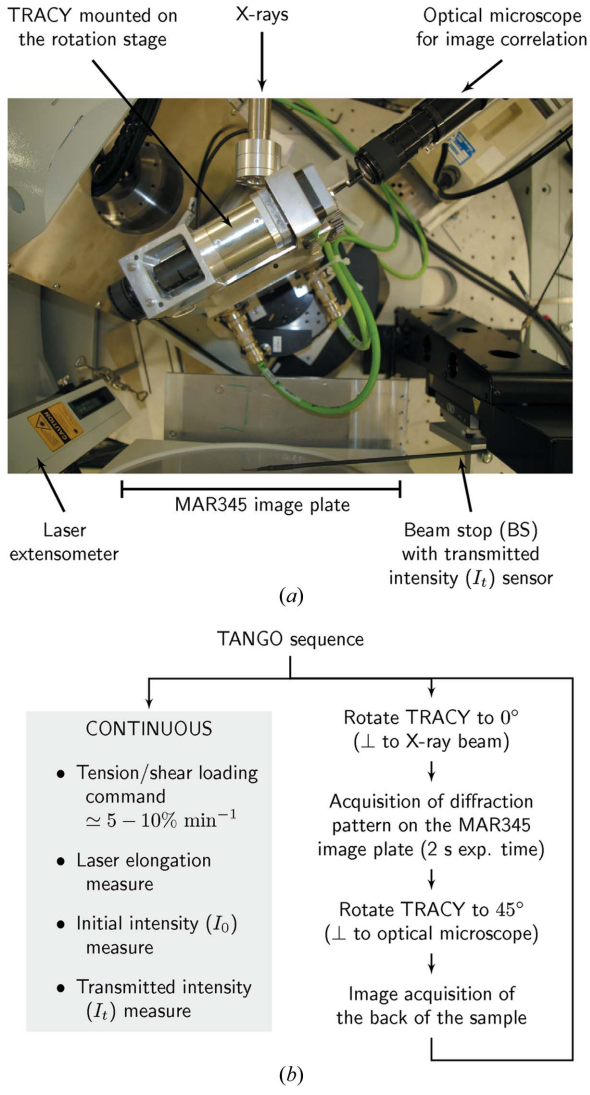

Figure 2
(*a*) Top view of the loading stage mounted on the DiffAbs diffractometer. Specimen elongation is measured by the laser extensometer, and the CCD camera is used to image the back of the sample during shear loading. (*b*) Flowchart detailing the *TANGO* sequence of the whole loading and acquisition process.

4. Application to *in situ* X-ray diffraction experiments

4.1. Experimental set-up

The present set-up has been used at the DiffAbs beamline to study NR crystallization under combined tension and shear. The NR specimen was illuminated with a monochromatic X-ray beam tuned at 7.8 keV. The beam monochromaticity ($\sim 10^{-4}$) is ensured by a double-crystal Si(111) monochromator (DCM). Two mirrors situated before and after the DCM are used for harmonics rejection ($\sim 10^{-5}$–10^{-6}) and vertical focusing of the X-ray beam. The second DCM crystal is also used as a sagittally focusing device to reduce the beam size and increase the photon flux at the sample position. The result is an X-ray beam of approximate size 300 µm × 300 µm (full width at half-maximum) at the sample position, with a photon flux of several 10^{11} photons s^{-1} in the X-ray spot.

An area detector (MAR345 image plate) is placed at ∼15 cm downstream of the sample. A Pb beamstop (BS) was used to block the intense transmitted beam through the NR sample. A Si diode placed in the centre of the BS served to record the transmitted beam intensity through the sample. From monitoring the X-ray beam intensities I_0 and I_t before and after the sample, respectively, it is possible to estimate accurately the thickness of the sample. This value can be used

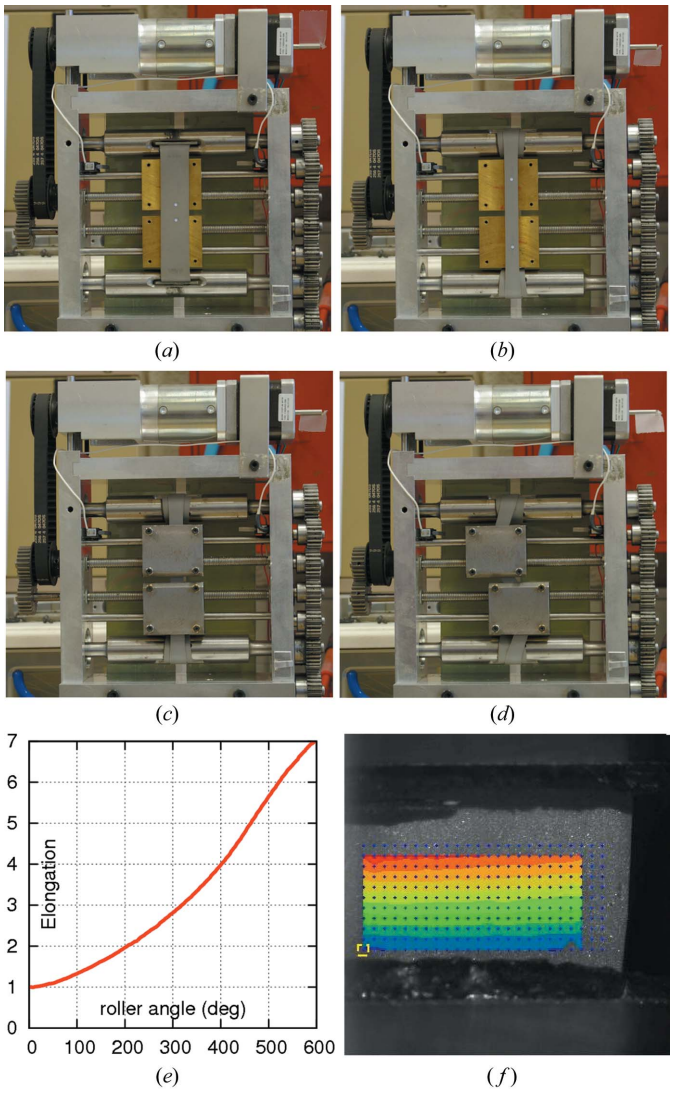

Figure 3
(*a*)–(*d*) Views of the specimen at different steps of the multi-axial test. (*a*) Unloaded specimen placed between tensile grips. (*b*) Elongated specimen during tensile loading. (*c*) Elongated specimen with shear grips positioned. (*d*) Stretched and sheared specimen during shear loading. (*e*) Calibration curve showing the specimen elongation as a function of the roller angle. (*f*) Image correlation carried out at the back of the sample to access the shear level.

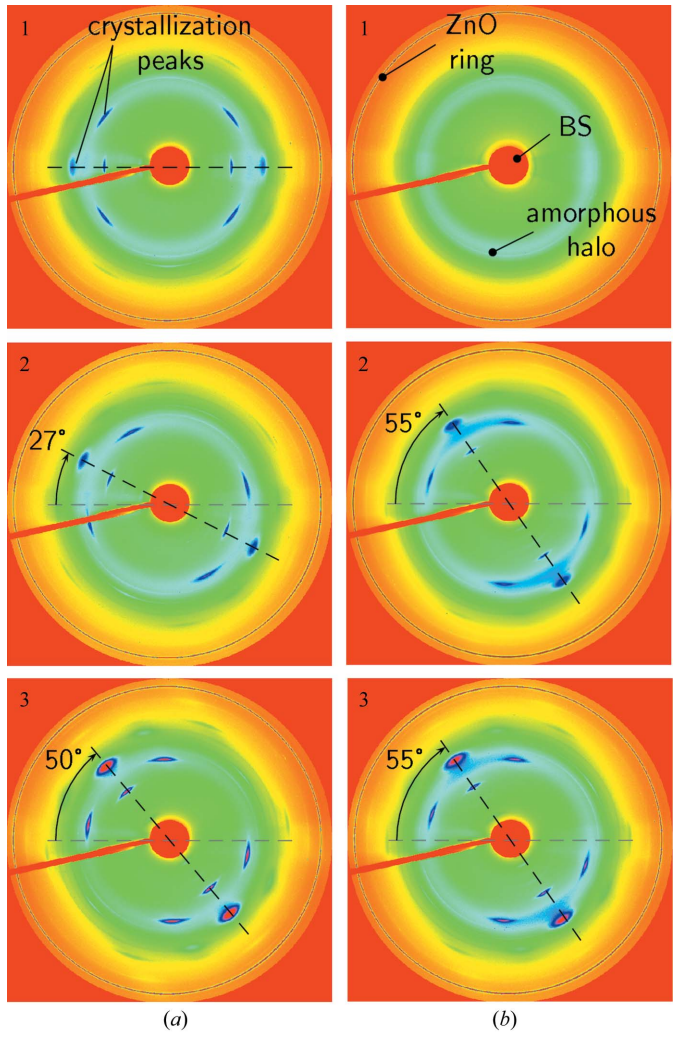

Figure 4
Two-dimensional WAXS characterization of NR material under combined tension and shear loadings. Figures in the left-hand column (*a*) describe experiment *A* where the sample is first stretched to 400% then sheared to 150%. Those in the right-hand column (*b*) refer to experiment *B* where the sample is stretched to 200% then sheared to 150%. (*a*1) WAXS pattern after 400% stretch showing crystallization. (*a*2) WAXS pattern after 400% stretch and 100% shear. (*a*3) WAXS pattern after 400% stretch and 150% shear. (*b*1) WAXS pattern after 200% stretch (no crystallization). (*b*2) WAXS pattern after 200% stretch and 130% shear. (*b*3) WAXS pattern after 200% stretch, 150% shear + 5 min relax.

at a later stage in the analysis to normalize the diffracted intensity (as the tension progresses, less and less matter is probed by the X-ray beam which leads to a proportionally smaller diffracted intensity).

Two experiments, labelled as *A* and *B* in the following, have been conducted. In experiment *A* the sample is first stretched to a maximum elongation λ_{max} of 400% then sheared to 150%. In experiment *B* a second sample is stretched to 200% then sheared to 150%.

The non-elongated NR sample is first centred in the X-ray beam using the lateral translations of the diffractometer. The specimen was then stretched in tension from 0 to λ_{max} continuously while monitoring the elongation *via* the laser extensometer and recording WAXS patterns with the MAR detector every 2 min (see Fig. 4*a*). The tension velocity was about 5% per minute so that a WAXS pattern was recorded every 10% elongation. At this point the elongated specimen was clamped into the shear grips and sheared to the desired value (150% in our series of experiments). The displacement speed was 1 mm min^{-1}. WAXS patterns were also acquired every 2 min and snapshots of the back of the sample were recorded by the optical microscope in between each WAXS acquisition. The whole sequence was programmed and run using the *TANGO* software of the beamline, as shown in Fig. 2.

4.2. Analysis of WAXS patterns

Visual inspection of the diffractograms reveals several interesting features. Before any elongation is applied, and up

to 200% elongation (see Fig. 4*b*1), the amorphous halo is clearly visible and a diffraction ring corresponding to small randomly oriented ZnO crystallites also appears at $2\theta = 30^\circ$. The observation during elongation allows the crystallization threshold under uni-axial load at 220% to be readily confirmed. Beyond this elongation threshold the crystallization peaks show a continuous strengthening.

After a uni-axial elongation to λ_{max}, a shear load has been used to impose a multi-axial stress state. The recorded two-dimensional WAXS patterns capture the effect on the crystallites orientation. In experiment *A* the crystallization peaks induced by uni-axial loading clearly rotate with the imposed shear loading which means that the crystallite orientations change with the strain path. As seen by comparing Figs. 4(*a*1), 4(*a*2) and 4(*a*3), the orientation changes gradually with applied shear. This orientation change can be measured precisely and may be correlated with the strain measured within the sample.

In experiment *B* the shear load is superimposed to uni-axial deformation below the crystallization threshold. The shear strain level has been increased gradually and crystallization appeared around 130% directly at $\varphi = 55^\circ$ (see Fig. 4*b*2). With further shear applied up to 150%, crystallization peaks were observed to remain at the very same position. At this point the shear level was kept constant to study the relaxation phenomenon. An increasing diffracted intensity was observed which can clearly be seen in Fig. 4(*b*3); this corresponds to a reinforcing effect. Again, in this case, the rotation angle of the crystallization peaks did not change.

Finally it can be noted that the two final patterns from experiments *A* and *B* look similar. This would suggest that the same crystallite organization can be achieved with different loading paths, although transverse orthotropy still needs to be verified to conclude, which appears difficult with the present set-up. This has been demonstrated for uni-axial loading but not yet in the general case.

To analyze further the X-ray diffraction data, the intensity can be integrated in the form of radial profiles. The crystallinity index can be determined using the simplified method of Mitchell (1984), which has been applied in several studies. It has been shown that the different phases could be deconvoluted to distinguish the amorphous phase from crystallites. Then the mass fraction and orientation of the crystalline phase can be retrieved as a function of the imposed elongation and shear levels. This information is essential to serve as input in multi-axial material constitutive behaviour.

One of the main limits of the present set-up was the long readout time of the detector. This can be improve in the future by using much faster detectors such as the hybrid-pixel detector XPAD now available at Soleil (Bérar *et al.*, 2002; Medjoubi *et al.*, 2010). This would allow rate-dependent mechanisms to be observed in great detail, such as reinforcement during relaxation and crystallite rotation during shear.

5. Conclusion

We have presented a novel fixture which can be used to load NR-based materials into non-proportional tension plus shear loadings while monitoring the crystalline phase formation *in situ*. Elastomer specimens can be elongated by more than 500% in tension and sheared to 200%. Both strain levels can be measured, *via* a laser extensometer for tension and using DIC for the shear level. The device is fully automated and can be operated using typical *TANGO* software allowing intimate links between loading and acquisition of X-ray diffraction patterns. One of the future improvements will be to monitor the elongation based on the laser extensometer measure to impose a constant strain rate and use a faster detector to follow rapid changes in the crystalline organization of the material. Further use of this machine will be the study of oligocyclic fatigue with soft materials.

All the experiments reported here were performed at Synchrotron Soleil (France) on the DiffAbs beamline. We would like to thank F. Alves for technical and mechanical support in integrating the loading device on the diffractometer. The Soleil Computing and Electronics departments are acknowledged for support in interfacing the device to the *TANGO* control system. Y. Auriac and R. Cluzet are acknowledged for fruitful discussions on the design of TRACY.

References

Albouy, P.-A., Marchal, J. & Rault, J. (2005). *Eur. Phys. J. E*, **17**, 247–259.
Bérar, J.-F., Blanquart, L., Boudet, N., Breugnon, P., Caillot, B., Clemens, J.-C., Delpierre, P., Koudobine, I., Mouget, C., Potheau, R. & Valin, I. (2002). *J. Appl. Cryst.* **35**, 471–476.
Brieu, M. & Diani, J. (2007). *J. Test. Eval.* **35**, 364–372.
Flory, P. J. (1953). *Principles of Polymer Chemistry*. Ithaca: Cornell University Press.
Geandier, G., Thiaudiere, D., Andriamazaoro, R. N. R., Chiron, R., Djaziri, S., Lamongie, B., Diot, Y., Le Bourhis, E., Renault, P. O., Goudeau, P., Bouaffad, A., Castelnau, O., Faurie, D. & Hild, F. (2010). *Rev. Sci. Instrum.* **81**, 103903.
Gent, A. N. (1954). *Trans. Faraday Soc.* **50**, 521.
Marco, Y. & Chevalier, L. (2008). *Polym. Eng. Sci.* **48**, 530–542.
Medjoubi, K., Bucaille, T., Hustache, S., Bérar, J.-F., Boudet, N., Clemens, J.-C., Delpierre, P. & Dinkespiler, B. (2010). *J. Synchrotron Rad.* **17**, 486–495.
Mitchell, G. R. (1984). *Polymer*, **25**, 1562–1572.
Thomas, A. G. (1955). *J. Polym. Sci.* **18**, 177.
Toki, S., Hsiao, B. S., Kohjiya, S. & Tosaka, M. (2006). *Rubber Chem. Technol.* **79**, 460–488.
Trabelsi, S., Albouy, P. & Rault, J. (2004). *Rubber Chem. Technol.* **77**, 247–259.
Treloar, R. G. (1947). *Trans. Faraday Soc.* **43**, 277–284.